Monatshefte für Chemie 134, 693–719 (2003)
DOI 10.1007/s00706-003-0590-3

Monatshefte für Chemie
Chemical Monthly
Printed in Austria

Invited Review

Crystallization and Phase Stability of $CaSO_4$ and $CaSO_4$ – Based Salts

Daniela Freyer* and **Wolfgang Voigt**

Institut für Anorganische Chemie, TU Bergakademie Freiberg, D-09596 Freiberg, Germany

Received December 17, 2002; accepted January 10, 2003
Published online April 3, 2003

Summary. Calcium sulfate occurs in nature in form of three different minerals distinguished by the degree of hydration: gypsum ($CaSO_4 \cdot 2H_2O$), hemihydrate ($CaSO_4 \cdot 0.5H_2O$) and anhydrite ($CaSO_4$). On the one hand the conversion of these phases into each other takes place in nature and on the other hand it represents the basis of gypsum-based building materials. The present paper reviews available phase diagram and crystallization kinetics information on the formation of calcium sulfate phases, including $CaSO_4$-based double salts and solid solutions.

Uncertainties in the solubility diagram $CaSO_4$–H_2O due to slow crystallization kinetics particularly of anhydrite cause uncertainties in the stable branch of crystallization. Despite several attempts to fix the transition temperatures of gypsum–anhydrite and gypsum–hemihydrate by especially designed experiments or thermodynamic data analysis, they still vary within a range from 42–60°C and 80–110°C. Electrolyte solutions decrease the transition temperatures in dependence on water activity.

Dry or wet dehydration of gypsum yields hemihydrates (α-, β-) with different thermal and rehydration behaviour, the reason of which is still unclear. However, crystal morphology has a strong influence.

Gypsum forms solid solutions by incorporating the ions HPO_4^{2-}, $HAsO_4^{2-}$, SeO_4^{2-}, CrO_4^{2-}, as well as ion combinations $Na^+(H_2PO_4)^-$ and $Ln^{3+}(PO_4)^{3-}$. The channel structure of calcium sulfate hemihydrate allows for more flexible ion substitutions. Its ion substituted phases and certain double salts of calcium sulfate seem to play an important role as intermediates in the conversion kinetics of gypsum into anhydrite or other anhydrous double salts in aqueous solutions. The same is true for the opposite process of anhydrite hydration to gypsum. Knowledge about stability ranges (temperature, composition) of double salts with alkaline and alkaline earth sulfates (esp. Na_2SO_4, K_2SO_4, $MgSO_4$, $SrSO_4$) under anhydrous and aqueous conditions is still very incomplete, despite some progress made for the systems Na_2SO_4–$CaSO_4$ and K_2SO_4–$CaSO_4$–H_2O.

Keywords. Calcium sulfate phases; Gypsum; Hemihydrate; Solubility; Polyhalite.

* Corresponding author. E-mail: daniela.freyer@chemie.tu-freiberg.de
Dedicated to Professor *H. Gamsjäger* on occasion of his 70th birthday

Introduction

Calcium sulfate in form of anhydrite or gypsum represents the most abundant sulfate mineral in nature. Evaporitic deposits contain also various amounts of double or triple salt minerals like syngenite, $K_2SO_4 \cdot CaSO_4 \cdot H_2O$, glauberite, $Na_2SO_4 \cdot CaSO_4$, or polyhalite, $K_2SO_4 \cdot MgSO_4 \cdot 2CaSO_4 \cdot 2H_2O$. In connexion with its application as binder or building material much attention has been paid to the hydration–dehydration processes of calcium sulfate under various conditions.

A number of important industrial processes like the wet limestone-gypsum flue-gas desulfurization (FGD), production of phosphoric acid or phosphate fertilizers, desalination of brackish or seawater, hydrometallurgical production of zinc and copper, and recovery of natural gas and oil, are accompanied by crystallization of calcium sulfate phases. For more than half a century efforts have been directed toward the control of growth rate and morphology of gypsum crystals formed in these processes or the prevention of its growth (anti-scaling). Crystallization and transformation of the calcium sulfate phases are influenced in a complex manner by temperature, pressure, dissolved electrolytes or organics, and the presence of its own or other minerals. Knowledge of the respective phase diagrams and solubility data belong to the necessary prerequisites to investigate crystallization processes. Together with kinetic information and structural relations between important phases, a basis for mechanistic understanding and control of crystallization would be provided. It is the aim of this review to summarize such information and to point out deficiencies. Thereby, the scope is broadened to related systems and conditions, where certain calcium sulfate containing phases can be formed.

System $CaSO_4$–H_2O

Phases and Structures

In contact with water three phases of calcium sulfate can crystallize: gypsum, anhydrite, and hemihydrate. Their main structural features are illustrated in Fig. 1. Common structural motif in all $CaSO_4$ phases are chains in the form [–Ca–SO_4–Ca–SO_4–], where sulfate tetrahedra are coordinated through oxygen atoms with two neighbouring Ca ions in chain direction.

Gypsum is distinguished by a marked layer structure with perfect cleavability parallel to (010), where the sheets of coordinated water are located. Vibrational spectroscopy revealed a pressure-induced phase transition in gypsum structure at approx. 5–6 GPa caused by water disorder [1].

In the hemihydrate structure the Ca^{2+}–SO_4^{2-}-chains run along the c-axis and form channels of approx. 4 Å diameter hosting the water molecules (Fig. 1b). Symmetry is near a threefold screw axis. Deviations are obviously correlated with water content as discussed below. Water molecules can obviously be replaced by other small molecules like methanol [2]. By means of careful drying of hemihydrate the water can be removed almost quantitatively, which yields the so-called soluble anhydrite (also denoted as AIII phase or γ-$CaSO_4$) with hexagonal symmetry.

The structure of the thermodynamic stable orthorhombic anhydrite (AII, insoluble anhydrite) contains the Ca–SO_4–Ca chains oriented in direction of the

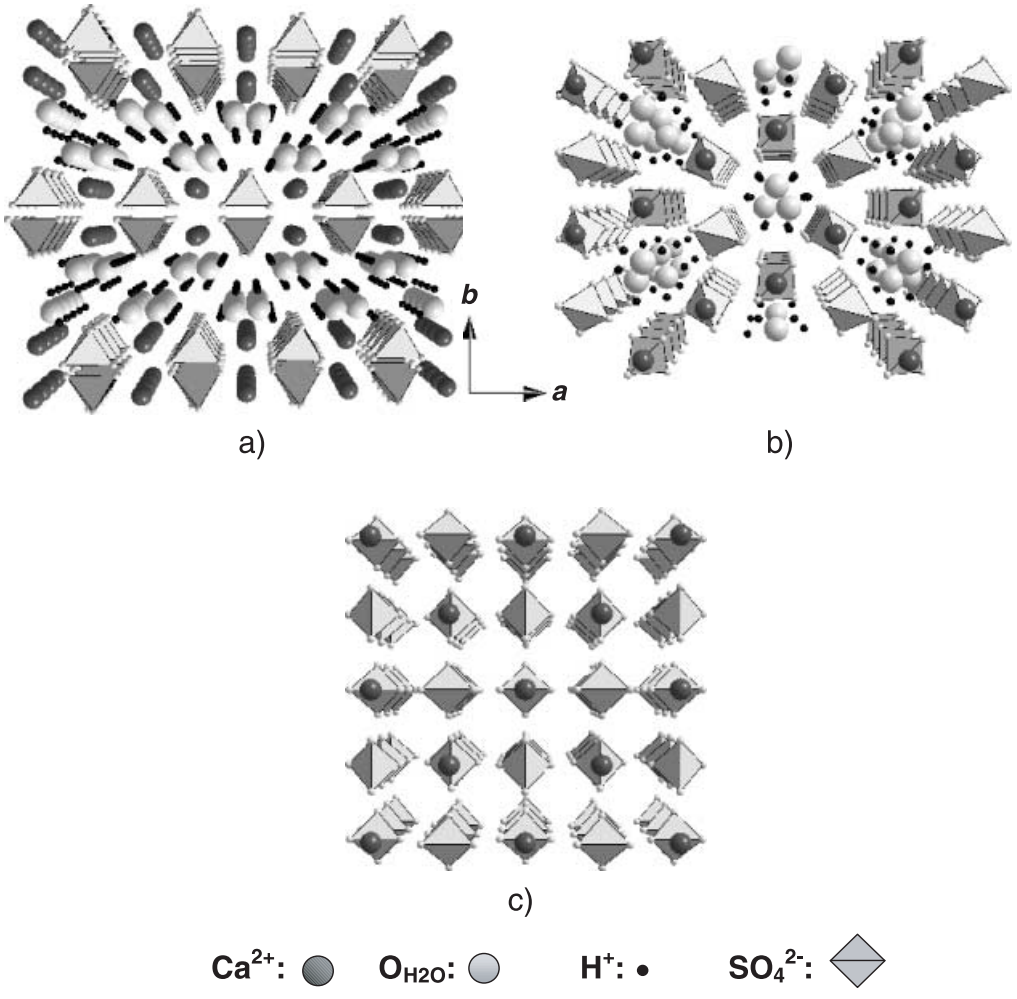

Fig. 1. Structures of a) gypsum, b) hemihydrate, and c) insoluble anhydrite with view in *c*-direction

shorter c-axis. In a- and b-direction these chains are corner-linked as illustrated in Fig. 1c.

Solubility Diagram – Thermodynamic Force of Transformations, Temperature Dependence

In Fig. 2 the solubility curves of the three phases gypsum, anhydrite, and hemihydrate are plotted in the temperature range 0–200°C at saturation pressure. At a given temperature the solid phase with the lowest solubility represents the stable phase. At low temperatures this is gypsum, at high temperatures it is anhydrite. Hemihydrate remains metastable at all temperatures. Due to slow crystallization kinetics the solubility determinations of a given solid can be extended into the metastable temperature range when nuclei of the stable phase are absent. Intersections of these curves yield the transition temperatures gypsum–anhydrite and gypsum–hemihydrate. Both temperatures are of considerable importance for the

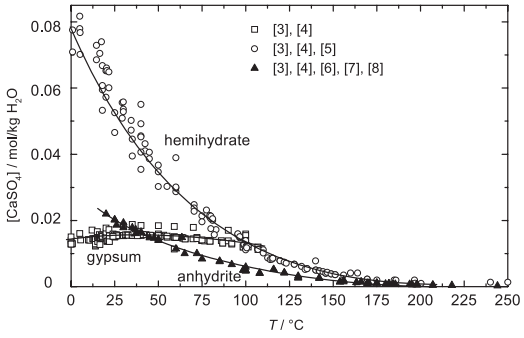

Fig. 2. Literature data of solubility of gypsum, anhydrite, and hemihydrate in the temperature range 0–200°C at saturation pressure

geology of evaporites (gypsum–anhydrite) or the production and application of gypsum products (gypsum–hemihydrate). As can be seen from Fig. 2 the data are considerably scattered and thus the intersection points vary depending on selected data.

Discussion of the transition temperature gypsum–anhydrite has a long history with changing opinion about its correct value. Most of the difficulties in this respect arise from the fact that anhydrite does not crystallize in water with measurable rate at temperatures below 70°C, even in presence of anhydrite seed crystals. Thus, the solubility equilibrium of anhydrite cannot be proved by approaching from both sides, that is, from under- and supersaturation.

In Fig. 3 the relevant part of the solubility diagram is enlarged and it can be seen that the borderlines of the data points yield transition temperatures from about 25–52°C.

However, the first value proposed by *Van't Hoff et al.* [9] at T=63°C was even higher and was derived from dilatometric investigations and thermodynamic considerations. This value was essentially accepted until the review on solubility equilibria of the oceanic salt systems prepared by *D'Ans* [3]. *Hill* [6] and *Posnjak* [10] determined the solubility carefully and argued that the transition temperature should be much lower, that is at 42±2°C. In a revised critical discussion *D'Ans et al.* [4] supported this view by including their own solubility data and

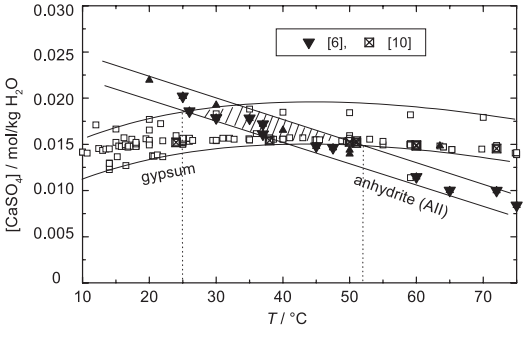

Fig. 3. Relevant enlarged part of the solubility diagram (Fig. 2) for transition temperature gypsum–anhydrite, values of *Hill* [6] and *Posnjak* [10] are marked

thermodynamic modelling. The differential dissolution enthalpies of gypsum derived from the temperature dependence of solubility agreed within $1.6\,kJ\cdot mol^{-1}$ with enthalpy measurements by *Lange et al.* [11], which *D'Ans et al.* [4] took as additional support for the lower transition temperature. In 1967 *Hardie* [12] published results of an extensive work to decide the question of gypsum–anhydrite conversion. He used a reaction approach. Gypsum, anhydrite, or their mixtures were suspended in sulfuric acid or sodium sulfate solutions of a certain water activity at constant temperatures between 20–70°C for 20 to 300 days. After the experiments X-ray patterns were recorded and from the intensity ratio of one typical reflex the degree of conversion was determined. An extrapolation of a plot conversion temperature versus water activity from solutions with lower water activities to pure water yielded a transition temperature of 58±2°C. Although *D'Ans* [7] replied very decisively against the statement of *Hardie* [12], it seems that this temperature is presently considered as more or less correct. In a more recent thermodynamic analysis of the system $CaSO_4$–NaCl–H_2O *Raju et al.* [13] claim agreement with this value. For the calculation of the Gibbs energy, ΔG, of reaction (I) the authors used solely thermodynamic standard data from sources [14] and [15].

$$CaSO_4\cdot 2H_2O(s) \Rightarrow CaSO_4(s) + 2H_2O(l) \qquad (I)$$

ΔG passes zero at T=60°C. Unfortunately, it was not exactly stated which data from which source had been selected. Nevertheless *Knacke and Gans* [16] pointed out that they corrected the standard entropy of anhydrite in [17] by $1.6\,J\cdot mol^{-1}\cdot K^{-1}$ in order to fit the transition temperature gypsum–anhydrite of 55.5±2°C, determined by themselves in a particular experiment. Thus, the transition temperature calculated from tables of standard thermodynamic data is not independent on solubility data.

In our opinion, the presently preferred transition temperatures between 55–60°C have no more justification than the lower values between 42–45°C. From both experimental studies [12, 16] higher transition temperatures are not beyond doubt. The high extrapolated temperature in the water activity-temperature plot used by [12] is fixed by five experiments between 50 and 55°C, in which reaction of anhydrite to gypsum was observed, however, with one exception not to completion. There were also runs with unexpected results. From the description of the experimental part it becomes clear that the water activity was not constant during the experiment, since approx. 100 g of sulfate were obviously suspended in approx. 100 g sulfuric acid solution. Thus, depending on the reaction (hydration or dehydration) solution concentration and hence the water activity will change.

Knacke and Gans [16] designed a clever experiment exploiting the fact that in a mixed suspension of anhydrite and gypsum the solubility is exclusively controlled by gypsum with the much faster crystallization kinetics. Thus, they were able to agitate anhydrite over a period of 3 months at temperatures near the assumed transition point gypsum–anhydrite. Above the transition temperature gypsum is metastable and its solubility is higher than that of anhydrite. Consequently, addition of gypsum causes dissolution of gypsum, which was detected by a corresponding increase of electrical conductivity. The opposite effect, decrease of electrical conductivity, was observed below the transition temperature. In this way the

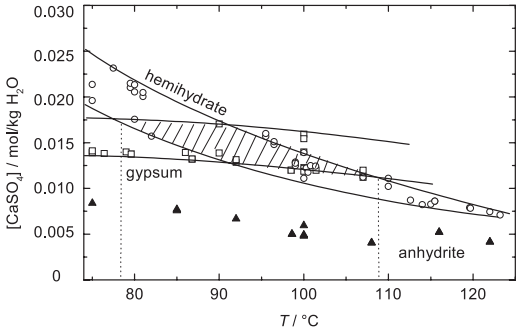

Fig. 4. Relevant enlarged part of the solubility diagram (Fig. 2) for the metastable transition temperature of gypsum–hemihydrate

transition temperature was fixed at 55.5±1.5°C. However, in their figure the conductivity of the solution obviously increases over the whole period of the experiment (two and three months, respectively). Assuming proportionality between conductivity and dissolved $CaSO_4$ concentration the increase is more than 6%. Reported anhydrite dissolution kinetic data [4, 6] show that constant concentration within 1–2% of the value is reached after 20–30 days. Also in cases where experiments lasted up to several months [6] no further concentration change was found. Thus, the reason for the conductivity increase remains unclear and consequently the conclusions drawn from the experiments must be questioned.

In Fig. 4 the crossing region of the solubility curve of gypsum and hemihydrate is shown. Within the scatter of the solubility data the possible transition temperature gypsum–hemihydrate covers a range from less than 80 to nearly 110°C. From their dilatometric and tensiometric experiments *Van't Hoff et al.* [9] derived 106°C as transition temperature. This value was accepted until *Posnjak* [10] critically analysed the work of *Van't Hoff et al.* [9]. *Posnjak* [10] derived a transition temperature of 97±1°C from solubility data and supported this value by means of a particular experiment, in which he observed complete conversion of gypsum into large hemihydrate crystals in pure water at a temperature below 100.5°C within two days.

Influence of Electrolytes on Transformation Temperature

There are numerous data on the solubility of gypsum in electrolyte solutions [18, 19]. More recent solubility determinations and discussion of trends can be found in [20–23]. In general the addition of non-common ion electrolytes enhances the solubility and can reach the tenfold value of the pure gypsum solution. With increasing electrolyte concentration the gypsum solubility surpasses a maximum value. The decrease of solubility at high electrolyte concentrations correlates obviously with the hydration ability of the electrolyte [23]. Most frequently the influence of NaCl was investigated. In this case both gypsum and anhydrite solubility were studied. In Fig. 5 data for T=25°C are plotted. The two solubility curves intersect at a NaCl content of approximately $4\,\mathrm{mol \cdot kg^{-1}}$ H_2O. Below this concentration gypsum represents the stable solid, above anhydrite. In a solution saturated with NaCl the transition temperature gypsum–anhydrite was estimated to

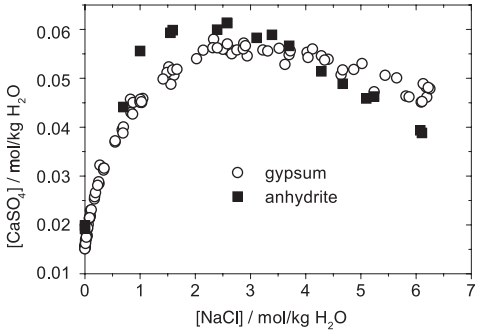

Fig. 5. Solubility of gypsum and anhydrite in dependence on sodium chloride concentration at T=25°C

18°C [4, 12]. Different authors more or less agree about this temperature. The reason may be seen in a faster equilibration in concentrated salt solutions.

For a comparison of the effects of various electrolytes on the shift of the gypsum–anhydrite transition only the water activity of the solutions has to be considered, given that the interaction between electrolyte and calcium sulfate does not yield new solid phases. From the dehydration reaction (I) and the appropriate expression of the *Gibbs* energy of this reaction, ΔG [Eq. (1)], it follows that the transition temperature decreases with decreasing water activity.

$$\Delta G = \Delta G^{\emptyset} - 2\mathrm{R}T \cdot \ln a_{\mathrm{W}} = 0 \tag{1}$$

For a given temperature function of $\Delta G^{\emptyset}$ the iterative solution of Eq. (1) provides the transition temperature as a function of water activity. Applying the standard data used by *Raju et al.* [13] a curve as given in Fig. 6 is obtained. The vertical line depicts the water activity of a saturated NaCl solution (a_{w}=0.75), which is quite temperature independent. Thus, with the $\Delta G^{\emptyset}$ function of *Raju et al.* [13] a transition temperature of about 32°C is calculated, which is much too high. Recorrecting the $1.6\,\mathrm{J{\cdot}mol^{-1}{\cdot}K^{-1}}$ entropy adjustment introduced by *Knacke and Gans* [16] to the standard data of *Barin et al.* [17] results in a transition temperature closer to the accepted value (see Fig. 6).

The influence of electrolytes on the transition temperature gypsum–hemihydrate can be discussed in a similar way. For a saturated NaCl solution a transition

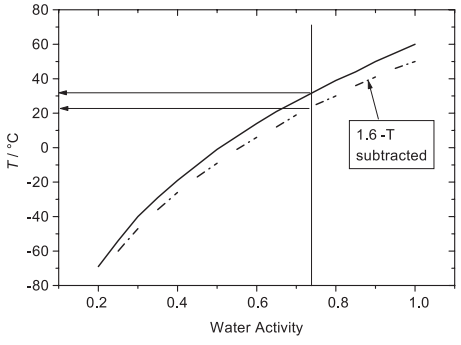

Fig. 6. Transition temperature gypsum–anhydrite derived from *Raju et al.* [13]

temperature of 76°C was estimated from vapour pressure data in [4], which at least does not contradict the experimentally observed conversion of gypsum into hemihydrate at 83 [4] and 75°C [24]. With solutions of lower water activity, such as of $MgCl_2$(aq.) or concentrated strong acids (*e.g.*, HNO_3) hemihydrate can be formed from gypsum near room temperature, which is exploited in preparative work. However, to our knowledge no systematic study or thermodynamic analysis of the hemihydrate formation in solutions of low water activity and temperatures has been undertaken.

Pressure Dependence

The solubility of all $CaSO_4$ phases increases with pressure. *Monnin* [25, 26] performed a detailed thermodynamic analysis of the pressure effect on solubility including the interaction with major sea water components over a broad temperature range. Another thermodynamic model of the pressure effect at 25°C was developed by *Krumgalz et al.* [27]. Increase of solubility with pressure is higher for anhydrite than for gypsum, which must cause a shift in transition temperature gypsum–anhydrite. *Mac Donald* [28] estimated an increase by 8 K if pressure is raised by 500 bar. No such estimations exist for the formation of hemihydrate. High pressure experiments of *Krüger et al.* [29] up to 6 GPa and 400°C gave no evidence for enhanced thermodynamic stability of hemihydrate with respect to anhydrite.

Crystallization of Gypsum

Nucleation, Crystallization Kinetics, and Morphology

Induction period measurements with an optical technique [30] at relative supersaturations of 1–4 and temperatures between 25–90°C resulted in an apparent energy of activation for nucleation ($30\,kJ{\cdot}mol^{-1}$) and an interfacial tension of $37\,mJ{\cdot}m^{-2}$. Supersaturation was generated by mixing Na_2SO_4 and $CaCl_2$ solutions of appropriate concentrations. Logarithmic plots of induction time versus supersaturation allowed to distinguish between homogeneous and heterogeneous nucleation mechanisms.

He et al. [31] determined the induction times by means of turbidity combined with sampling of solution and titrating Ca^{2+} concentration with *EDTA* in NaCl solutions up to $6\,mol{\cdot}kg^{-1}$. Whereas *Lancia et al.* [30] found no temperature dependence of the interfacial tension, *He et al.* [31] reported increasing values with temperature from $39\,mJ{\cdot}m^{-2}$ at 25°C to $64\,mJ{\cdot}m^{-2}$ at 90°C. NaCl has a strong influence on gypsum nucleation [31–33]. Interestingly, the variation of induction times with NaCl concentration is opposite to the trend of gypsum solubility in dependence on NaCl concentration [31]. That is, shortest induction times are observed at $3\,mol{\cdot}kg^{-1}$, where the solubility of gypsum passes a maximum, and therefore concentration supersaturation is lowest. It could be demonstrated by the authors that the induction period is correlated with the interfacial tension, which decreases with solubility. An activation energy of nucleation of $53\,kJ{\cdot}mol^{-1}$ was calculated from the temperature dependence at 3 *M* NaCl.

In a subsequent paper of *He et al.* [34] on growth kinetics no induction period was reported when seeding with 0.5–4 g of gypsum per kg of water. *Hina et al.* [35] investigated the crystallization kinetics of gypsum in dependence on the molar Ca^{2+}/SO_4^{2-} ratio in solution. The growth rate decreased with increase of this ratio. With KCl as supporting electrolyte the effect was stronger than with NaCl. In NaCl solutions the growth rate was generally lower than in KCl solutions. The effect does not correlate with variations in the thermodynamic driving force with solution compositions. Sodium ion adsorption was suggested as a reason for kinetic retardation. More drastic growth retardation is reported when La^{3+}, Ce^{3+}, and Eu^{3+} ions are present [36]. Lanthanum, which has the largest effect, reduces the growth rate by a factor of 10 already at concentrations of $3 \cdot 10^{-4} M$.

In the presence of inhibiting additives like phosphonates (*ENTMP*, *TENTMP*) an induction period is observed [37] even in seeded solutions. Growth kinetics after the induction period is nearly the same as in solutions without additives and no change in morphology could be detected. From these facts it was concluded that the inhibitors are adsorbed at the gypsum surface and incorporated by overgrowth.

The kinetics of gypsum crystallization from anhydrite suspended in water at 10–40°C was investigated by *Kontrec et al.* [38]. Under the conditions chosen (few grams of solid per dm^3 solution) transformation kinetics was dependent on both dissolution kinetics of anhydrite and growth of gypsum. The authors derived a kinetic model for this interdependence from their experimental data.

Influence of *PA*Na on homogeneous and heterogeneous nucleation was investigated by *Boisvert et al.* [39]. They found blocking of gypsum nucleation as the controlling factor on the kinetics of hemihydrate to gypsum conversion.

Bertoldi [40] tested a long list of organic and inorganic additives on their influence on crystal size and shape, however, no definite conclusions had been drawn with respect to certain additives. *Konak* [41] carried out similar experiments but did not report much about experimental details. For Separan (polyacrylamide) he stated a pronounced retardation in crystallization and growth of aggregates consisting of long, needle-shaped crystals [41]. Effects of additives on morphology and texture were also examined by *Amathieu et al.* [42]. They tested the influence of malonic, tartaric, and polyacrylic acid, as well as sodium tripolyphosphate, sodium laurylsulfate, dodecylammonium chloride, and ammonium sulfate. Attempts to correlate texture changes with strength of the final gypsum product is not straight-forward. Thus, large crystals can generate large and also low strengths. In a more recent study [43] the influence of malic acid, citric acid, tartaric acid, and adipic acid on gypsum crystallization kinetics and morphology from suspended hemihydrate was investigated. Also the adsorption of adipic and rac-malic acid was measured by capillary zone electrophoresis. Largest effects were observed for citric acid and malic acid. The results were explained by positional matching of the acids' oxygen with the Ca^{2+} distances on the (120) and (–111) crystallographic planes on gypsum.

From texture analysis *Follner et al.* [44] conclude that after setting of α-hemihydrate at a low water/gypsum ratio there is a tendency of parallel orientation of the (010) faces of gypsum with (100) faces of hemihydrate. No preferred orientation of gypsum formed from hemihydrate at water/solid ratios between 0.50 to 1.50 was observed in time-resolved synchrotron X-ray powder diffraction experiments [45].

Hydration of anhydrite into gypsum is accelerated by certain acids, bases, and salts. Alkali sulfates are the most effective. In dilute solutions hydration proceeds *via* transient complexes. The formation of complexes is believed to be a surface ionic transfer process. Depending upon temperature and concentration double salts can be formed [46].

Ion Substitution in Gypsum and Related Phases

Kushnir [47] investigated the co-precipitation of Na^+, K^+, Mg^{2+}, and Sr^{2+} with gypsum and determined distribution coefficients in dependence on concentration between 30–50°C. No extensive incorporation is observed for Na^+, K^+, and Mg^{2+} with values of D (x_G/x_{Brine}) in the range of 10^{-5} to $3 \cdot 10^{-4}$ but a correlation with the growth rate of gypsum is found. The value for Sr^{2+} is between 0.2 to 0.7, which is much higher, but because of the low solubility of $SrSO_4$ the absolute amounts of incorporated Sr^{2+} are very small. Uptake of Cd^{2+} during gypsum crystallization from dilute solutions was determined but no specific effects could be found [48].

Extensive solid solutions are formed with HPO_4^{2-} ions. The mineral brushite, $CaHPO_4 \cdot 2H_2O$, is structurally very similar to gypsum, although proton ordering lowers the symmetry to *Ia* [49], whereas the gypsum structure is described with $I2/c$. Thus, an isodimorphic series of mixed crystals was found from inspection of IR spectra and X-ray powder patterns [50]. According to these authors up to 70 mass-% $CaHPO_4 \cdot 2H_2O$ can be incorporated into the gypsum structure. Consequently the mineral ardealite, $CaSO_4 \cdot CaHPO_4 \cdot 4H_2O$, should be considered as a gypsum based mixed crystal formulated as $Ca(SO_4)_{1-x}(HPO_4)_x \cdot 2H_2O$ with $x \approx 0.5$ [50]. This view is supported by the site occupation factors of 0.5 for sulphur and phosphorus in a crystal structure analysis [51].

At a pressure of 2.1 GPa pure brushite undergoes a phase transition [52]. In a more recent crystallization study in the gypsum–brushite system stable mixed crystals were only obtained from solutions with at least 30% phosphate. From solutions with 10–20% phosphate mixed crystals appeared as the first phase, then gypsum precipitated and the mixed crystals dissolved. When gypsum crystallized alone it did not contain any detectable amounts of phosphate [53]. Kinetic experiments have shown that brushite may serve as an effective nucleator in gypsum crystallization [54].

The dehydration of $CaHPO_4 \cdot 2H_2O$ differs from that of gypsum, an adequate hemihydrate is not known [55]. Monosodium phosphate, NaH_2PO_4, can also be incorporated into the gypsum lattice [56]. Calcium hydrogen arsenate also forms a dihydrate with a gypsum analog structure [57]. However, no detailed studies of arsenate uptake by gypsum are available.

The dihydrate of calcium selenate crystallizes also in a gypsum type structure with space group $I2/a$ [58] and lattice constants very similar to gypsum, however, its solubility is more than ten times higher [59]. Thermal dehydration is similar to gypsum with formation of an intermediate hemihydrate at approx. 137°C [60]. One should expect a continuous series of isomorphic mixed crystals between these two dihydrates, however, experimental investigations about this subject could not be found in literature.

Double substitution of Ca^{2+} and SO_4^{2-} by trivalent lanthanide and phosphate is realized in the mineral churchite, $[Y_{(1-x)}(Gd, Dy, Er)_x]PO_4 \cdot 2H_2O$, which is also isomorphous with gypsum [61].

Interestingly, the crystal structure of $CaCrO_4 \cdot 2H_2O$ is quite distinct from gypsum [62], although there exists an unstable monoclinic polymorph, which is described as isomorphous with gypsum [63].

Another mineral related to gypsum represents the recently discovered rapidcreekite [64]. Lattice symmetry and dimensions are different compared with gypsum. However, its structure can be derived by replacing every second sulfate row in gypsum lattice by carbonate anions.

Calcium Sulfate Hemihydrate and Related Phases

Formation, Morphology, and Properties

Hemihydrate occurs in nature as the mineral bassanite. Recently, it was also discovered in statoliths of a deep-sea medusa [65]. Generally hemihydrate can be prepared from gypsum by drying at enhanced temperatures, the product obtained by this way is denoted as β-hemihydrate [66–71]. The dehydration reaction is described as a topotactic solid state reaction, thereby it is suggested that the original [010] or [001] crystal axis of gypsum becomes the new [001] of the hemihydrate [72, 73]. In the dry system a stable T-p_{H_2O} region exists for the hemihydrate, which was carefully investigated recently [74, 75].

In aqueous solutions, hemihydrate can be crystallized as a metastable phase, because of the low crystallization rate of the stable anhydrite. The products prepared from aqueous solutions are denoted as α-hemihydrate. Normally, a suspension of gypsum is heated above the transformation temperature. The latter depends on the water activity as discussed earlier. Passing the transition temperature, gypsum in an aqueous suspension will be converted spontaneously into hemihydrate, which crystallizes in typical aggregates of hexagonal columns. The transformation of gypsum into α-hemihydrate is described as a topotactic solid state reaction in case of gypsum single crystals only. The transformation takes place under retention of the crystallographic c-axis [76, 77]. For polycrystalline gypsum the dominant mechanism is the dissolution of gypsum and generation of a supersaturation with respect to hemihydrate followed by nucleation of hemihydrate and growth of nuclei to macroscopic crystals from solution or on the surface of mother gypsum crystals without directional correlation [76, 78]. In dependence on the history of the gypsum used (formation, crystal size, impurities, ...) the mechanism of crystallization is supplemented by the topochemical reaction in a certain degree. A deeper understanding of governing mechanisms is necessary to control crystal form and sizes as an important issue in the production of special gypsum binder, where the control of hemihydrate morphology is effected by organic and inorganic additives. A review about significance and operating mode of different additives is given by *Koslowski et al.* [80]. More insight into the mechanistic steps could lead to a necessary comprehension of the effects of additives and their exploitation. Investigations on homogenous hemihydrate nucleation would be desirable in order to differentiate between solution sustained crystallization and the influence of hetero surfaces.

Table 1. Transformation of gypsum into hemihydrate in acid or salt solutions [66]

Electrolyte	$T/°C$
HNO_3 (60%)	50, 80
concentrated NaCl-solution	80
concentrated $MgCl_2$-solution	55

Table 2. Investigations on α- and β-hemihydrate properties

References	Investigated properties, methods	Main conclusion
[68, 81–83]	x-ray	– no basic differences of α- und β-HH[a)] – weaker reflexes for β-HH due to crystal size and lattice defect
[84–86]	surface	– very high specific surface of β-HH compared to α-HH
[81, 87–90, 91]	IR	– no differences between α- und β-HH – weaker bands for β-HH
[66, 68, 70, 82, 88, 91–95]	thermal behaviour	– controversial results (see text below)
[96, 97]	hydration heat	– lower heat of hydration for α-HH than for β-HH, the latter shows a wide variation in its hydration values
[98]	structure	– no differences
[44]		– differences between α- und β-HH
[99]		– α-HH monoclinic and β-HH trigonal

[a)] HH=hemihydrate

Such effects, *e.g.* the epitaxial growth of hemihydrate on fluorapatite was observed by *Dorozhkin* [79]. Different electrolytes show also influences on the α-hemihydrate morphology, where at least the lowered transition temperature gypsum–hemihydrate represents one factor one has to consider. Table 1 gives examples for hemihydrate formation experiments carried out by *Flörke* [66].

The α-hemihydrate differs in a number of properties (heat of solution, specific surface, solubility, effects in thermal analysis) from the β-form. There exist numerous papers dealing with these differences. In Table 2 some important articles are listed together with the investigated properties and main conclusion.

The dehydration of α- and β-hemihydrate takes place between 100–200°C depending on water vapour pressure followed by formation of soluble AIII and its transformation to insoluble AII, which occurs at different temperatures for α- und β-hemihydrate. The formation of AII is observed at temperatures between 200–600°C [66, 68, 70, 88, 92–94]. For β-hemihydrate *Kuntze* [69], *Powell* [82], and *Cliffton* [91] observed a weak exothermic effect at 350–375°C. The occurrence of an exothermic effect for α-hemihydrate at lower temperatures close to the dehydration is discussed controversially. *Budnikov et al.* [95] did not observe such an effect. In contrast, *Kuntze* [69] monitored an exothermic effect below 250°C. *Powell* [82] and *Cliffton* [91] found the exothermic effect between

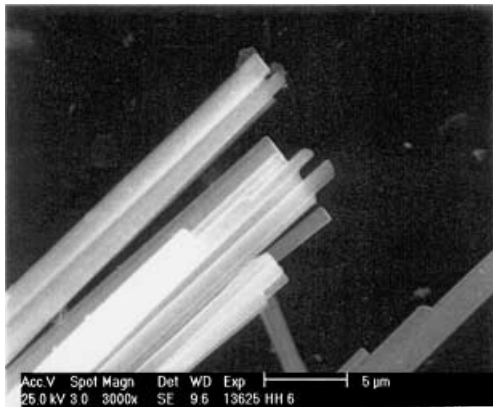

(7)

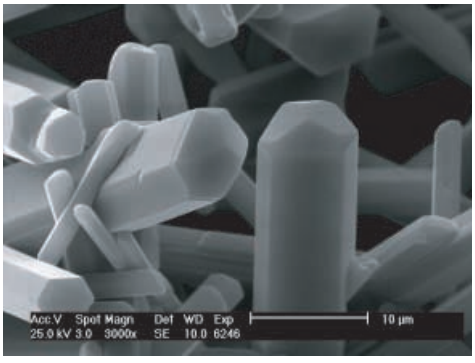

(8)

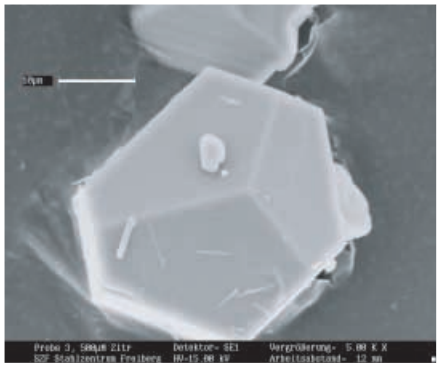

(9)

Figs. 7–9. Hemihydrate morphologies

163–255°C depending on the water vapour pressure. *Powell* [82] noticed different magnitudes of the effect for samples with different initial weights. The slower transformation at higher temperatures of the β-form is explained with a near relationship to AII [82, 92] but this assumption seems to be questionable.

Our own investigations on α- and β-hemihydrate show that the morphology (changes in surface conditions) of the samples has a large influence on the thermal behaviour [100]. Crystals of fibres (Fig. 7) show an apparently higher thermal stability. The dehydration takes place at some higher temperatures (100–160°C) compared with disk-like crystals (90–125°C) short along *c*-axis (Fig. 9). In

this morphology the water molecules have a short outlet way. The hemihydrate transformations were monitored by *in situ Raman* spectroscopy. A fast transformation to AIII was observed for stick-morphology (Fig. 8) in connexion with a sharp exothermic effect. Hemihydrate fibres transform very slowly into AIII, therefore the exothermic effect is not detectable. According to the exothermic effect for β-hemihydrate above 320°C the topotactical transformation to AII seems to be retarded in a certain manner by the pseudomorphosis to gypsum. Analogously, in the aqueous system the transformation of gypsum to AII is not a direct reaction. The intermediate formation of α-hemihydrate is the preferred reaction way. So, the topotactical transformation of a well crystallized α-hemihydrate compared with a gypsum-pseudomorphic β-hemihydrate is promoted. Probably, the contradictory discussions in literature result from different hemihydrate morphologies, among other things.

There are different conclusions in literature regarding water content and symmetry of hemihydrate. *Kuzel et al.* [98], *Bushuev et al.* [101], *Abriel et al.* [102], and *Oetzel et al.* [75] proposed that the water content and thus the symmetry varied depending on water vapour pressure ($CaSO_4 \cdot xH_2O$, $0.5 \leq x \leq 0.8$).

The so-called subhydrates are described with a trigonal space group *P 3$_1$21* [94, 98, 102, 103]. For $0.5 < x < 1$ a statistically disordered distribution of water molecules allows a deflection from their positions to reach the necessary distances. The pronounced anisotropy of the O_{H_2O} in the trigonal cell shows this fact [103]. For x=0.5 an ordered distribution of water molecules with a monoclinic cell is reached by doubling of the *c*-axis length [98, 104] whereas literature presents various structures (Table 3). Our earlier investigation [24] confirms a monoclinic lattice of the hemihydrate based on low temperature *Raman* spectroscopy.

The transition hemihydrate–subhydrate is demonstrated by small changes in the powder diffraction pattern [98, 104], also by *Oetzel et al.* [75]. They determined the vapour pressure–temperature condition in the solid–gas equilibrium for its

Table 3. Structure of $CaSO_4 \cdot 0.5H_2O$ proposed in literature

References	Lattice	Comment
[66, 105]	orthorhombic	
[66, 102], [44]	trigonal	deviations from the trigonal symmetry are small and that the different variants of occupying the crystallographically possible water positions cannot be distinguished by X-ray methods at present
[105]	hexagonal	
[98, 101, 104, 106], [107]	monoclinic, *C*2 or *I*2	strongly pseudo-trigonal, small deviations from trigonal structure arise from water molecules ordering inside the channels

existence. The term subhydrate is often used for hemihydrate without specified water content.

Ion Substitution – Sodium, Potassium, Strontium, and Rare Earth Cations

Sodium and Potassium

First hints for the inclusion of sodium ions in hemihydrate were given by *Hill et al.* [108]. A so-called sodium pentasalt, $Na_2SO_4 \cdot 5CaSO_4 \cdot 3H_2O$, is obtained when gypsum is stirred in sodium sulfate containing solutions at 75°C. Depending on temperature conversion is completed after 4 days up to one week [108, 109]. With the aim to prepare hemihydrate in sodium chloride solution a content of 2.3–2.9% sodium was found in the chloride free $CaSO_4 \cdot 0.5H_2O$ which is described by similar properties as the sodium pentasalt [96, 110].

The similarity of the X-ray powder diffraction pattern with the hemihydrate already suggests a hemihydrate structure, where Ca^{2+} is statistically substituted by Na^+. According to this explanation of the X-ray patterns one Na^+ ion replaces 1/6 of Ca^{2+} in the lattice. For charge compensation a second Na^+ is located statistically inside the structure. The discussions differ between a location within the $CaSO_4$ chain-matrix by distortions of sulfate tetrahedra or vacancy occupation and locations inside the water channel (Fig. 10) [89, 94, 110, 111].

Reisdorf et al. [94] denote Na-pentasalt as Na-polyhalite, although the name sodium polyhalite has been used already for a salt with the composition $3/5Na_2SO_4 \cdot 2/5K_2SO_4 \cdot 5CaSO_4 \cdot 3H_2O$ [112–113], which also has hemihydrate structure. Accepting this structural scheme one could expect a continuous series of solid solutions $CaSO_4 \cdot 0.5H_2O$–$(Na_{2x}Ca_{6-x})SO_4 \cdot 0.5H_2O$ [111]. Attempts to prepare such solid solutions from Na_2SO_4– or NaCl-containing solutions ended all the time very close to the pentasalt composition $Na_2Ca_6(SO_4)_3 \cdot 0.5H_2O$ or at sodium contents below $Na_{0.5}Ca_{5.75}(SO_4)_3 \cdot 0.5H_2O$ [109]. Thermal analyses support the view that sodium ions are located in the channels along the *c*-axis. As can be seen in Fig. 11 the dehydration temperature of the hemihydrate increases with sodium content. The highest dehydration temperature is observed for the potassium containing salt, which was first prepared by *Autenrieth* [112] and which he named "Na-polyhalite". In this ion substituted hemihydrate the sodium content is substituted partly by potassium. A proposed structure based on the X-ray diffraction pattern by *Gudowius et al.* [113] ascribed this salt also to the hemihydrate structure type. Its thermal behaviour fits into this view. The potassium ions substitute sodium ions in the channel, which causes a stronger hindrance for water molecules to leave along the channel [114].

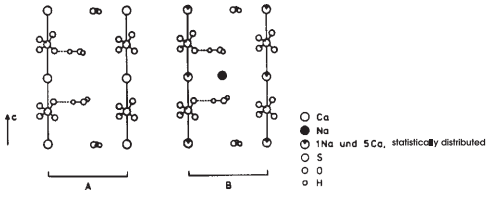

Fig. 10. Projection along the channel in hemihydrate structure (A) beside the analogous projection in the proposed pentasalt structure (B) [94]

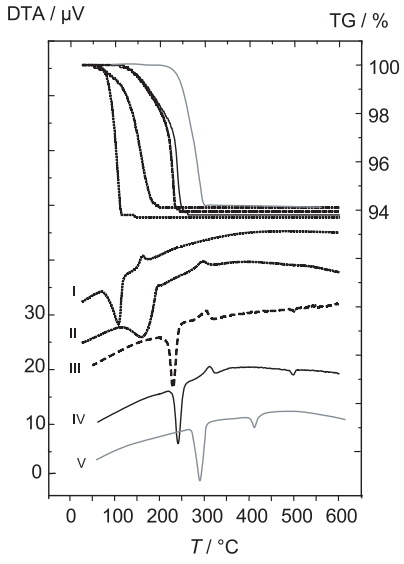

Fig. 11. TG/DTA of hemihydrate phases according to the compositions I–V [109, 114]; I $CaSO_4 \cdot 0.5H_2O$ ($6CaSO_4 \cdot 3H_2O$); II $0.23Na_2SO_4 \cdot 5.77CaSO_4 \cdot 2.95H_2O$; III $0.9Na_2SO_4 \cdot 5.1CaSO_4 \cdot 2.85H_2O$; IV $1.01Na_2SO_4 \cdot 4.99CaSO_4 \cdot 2.90H_2O$; V $(0.35 \pm 0.05)K_2SO_4 \cdot (0.55 \pm 0.05)Na_2SO_4 \cdot (5 \pm 0.05)CaSO_4 \cdot (3 \pm 0.05)H_2O$

Because of the possible substitution of ''channel''-sodium ions by potassium a substitution by ammonia ions in the same way can be expected in the hemihydrate structure. Crystal structure analysis from a small twin with sodium pentasalt composition yielded a superstructure of hemihydrate whereby one sodium position is found in the channel near the fourth unoccupied water position beside the sodium substituted Ca(2) position in the chain-matrix. For structural reasons the Ca(1) position is not substituted [109] (Fig. 12). Thus higher sodium contents in the hemihydrate enforce structural distortions, which gives rise to a discontinuity in solid solution formation. However, more extensive investigations will be necessary to determine the correlation between crystallographic parameters and composition of solid and aqueous solution.

Preparation of solid solutions between $CaSO_4 \cdot 0.5H_2O$ and $SrSO_4 \cdot 0.5H_2O$ and its identification by means of the X-ray patterns was reported [115, 116]. Precipitation of the sulfates from 0.5 *M* nitrate solution by adding 20% sulfuric acid at 90°C resulted in a maximum of 14 mol-% $SrSO_4$ in $CaSO_4 \cdot 0.5H_2O$ [116].

Rare Earth Cations

The ionic radii of the trivalent rare earth cations of the light lanthanides (La–Eu) are very similar to Ca^{2+}, for Ce^{3+} the values are nearly identical. Thus, isomorphic substitution of Ca^{2+} should be possible if suitable ions for charge compensation are available. *Bushuev et al.* [117] investigated the incorporation of Ce^{3+} into the hemihydrate according to two different substitution schemes I and II.

$$2\ Ca^{2+} \Leftrightarrow Ce^{3+} + Na^{+} \qquad \text{(I)}$$

$$Ca^{2+} + SO_4^{2-} \Leftrightarrow Ce^{3+} + PO_4^{3-} \qquad \text{(II)}$$

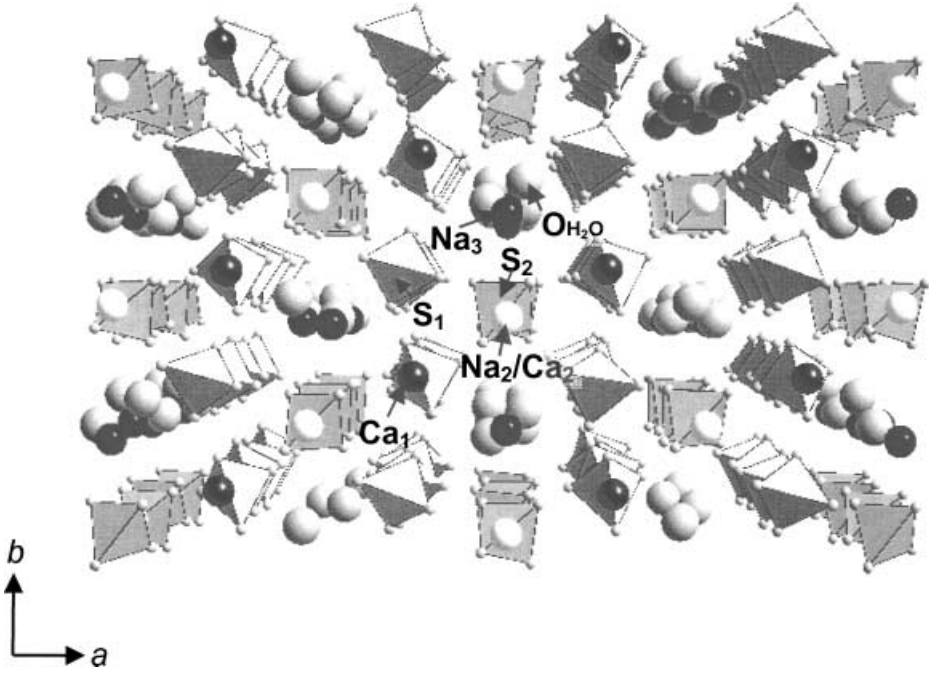

Fig. 12. Projection across the channel in Na-pentasalt structure [109]

Precipitation of the hemihydrates from nitrate solutions of suited compositions by adding sulfuric or phosphoric acid at 70–95°C yielded continuous series of solid solutions $CaSO_4{\cdot}0.5H_2O$–$Na_{0.5}Ce_{0.5}(SO_4){\cdot}0.5H_2O$ and $CaSO_4{\cdot}0.5H_2O$–$CePO_4{\cdot}0.5H_2O$. Existence of a solid solution phase was confirmed by recording the X-ray diffraction patterns and determination of the lattice constants, which varied smoothly with composition of the solid phase. Mixed crystals containing $Na_{0.5}Ce_{0.5}(SO_4){\cdot}0.5H_2O$ were of more isometric habitus. The hemihydrate analog structure was confirmed by crystal structure analysis for $Na_{0.5}Ce_{0.5}(SO_4){\cdot}0.5H_2O$ [118a] and $Na_{0.5}La_{0.5}(SO_4){\cdot}0.5H_2O$ [118b]. Sorption kinetics and distribution coefficients of Ce^{3+} and Eu^{3+} in solutions of 7.5 *M* H_3PO_4 and hemihydrate at 90°C have been determined using radioactive isotopes of the metal ions [119].

The complete series of isomorphous mixed crystals $NaLn(SO_4)_2{\cdot}H_2O$ (*Ln*=Y, La, Ce, ..., Yb, Pu) was prepared and characterised by X-ray diffraction [120]. A thorough thermal characterisation (TG, DTA, IR, X-ray) can be found in [121]. Since $NaPu(SO_4)_2{\cdot}H_2O$ is isomorphous to the corresponding rare earth sulfate monohydrates [120] the incorporation of Pu(III) into $CaSO_4$ phases with hemihydrate structure can be expected. Interestingly, no incorporation of Ce^{3+} into gypsum was observed. The ability of hemihydrate to incorporate lanthanide ions on one side and the inability of gypsum for this substitution on the other side is exploited for extraction of rare earth elements in phosphoric acid production from apatitic ores [122].

Anhydrite

In aqueous solutions, the crystallisation of anhydrite is the most difficult of all calcium sulfate phases and reports about its formation at temperatures below

100°C are contradictory. There exists agreement that below 90°C no spontaneous formation of anhydrite occurs. Dissolved salts facilitate anhydrite formation and solid–liquid equilibration. *Hill* [123] attempted to prepare anhydrite for dissolution experiments by boiling gypsum in electrolyte solutions. The final product after 1–3 days boiling was mostly hemihydrate. *Hill* [123] obtained successful conversion to anhydrite within 3 days in 5% K_2SO_4 or 15–20% H_2SO_4 solution. Crystal sizes of anhydrite were in the range of 20–30 μm. At 90.5°C gypsum was transformed through hemihydrate into anhydrite within 10 days in solutions containing NaCl or NaCl–$MgCl_2$ with chloride concentrations higher than 2.8 $mol \cdot dm^{-3}$ [124]. *Ostroff* [124] postulated that supersaturation with respect to hemihydrate is required to form anhydrite. Thus, in concentrated NaCl solution at 50 and 70°C anhydrite was not formed corresponding to the fact that in saturated NaCl solution hemihydrate is formed only above 80°C [4]. *Hardie* [12] argues that anhydrite is not formed through a solution-precipitation mechanism, because addition of anhydrite has no accelerating effect, also citing similar results from *Zen* [125]. However, both authors reported unexpected experimental results of gypsum formation from anhydrite under conditions where anhydrite should have been stable. Hydration of anhydrite to gypsum is also kinetically hindered. Without gypsum seed crystals anhydrite can be agitated in solutions several months without any change [12, 16].

Calcium Sulfate-Based Double Salts

Double Salts with Sodium Sulfate

In the anhydrous system the appearance of the compounds $4Na_2SO_4 \cdot CaSO_4$, $Na_2SO_4 \cdot CaSO_4$ (the mineral glauberite), and $2Na_2SO_4 \cdot CaSO_4$ is discussed controversially. *Calcagni et al.* [126] suppose a $3Na_2SO_4 \cdot CaSO_4$ phase with a melting point at 949°C. Different versions of phase diagrams exist [127–130]. The reasons have to be seen in the tendency of high temperature forms of sodium sulfate to coexist at low temperature in metastable equilibrium. Thus, the phase diagrams reflect kinetic situations but not equilibrium. In *Freyer et al.* [131] the formation and transformation of metastable into stable phases is investigated thoroughly and the equilibrium phase diagram is derived (Fig. 13). Glauberite is the only stable anhydrous compound of sodium and calcium sulfate and will decompose above 520°C. The phase $4Na_2SO_4 \cdot CaSO_4$ [127] is part of a solid solution series of the hexagonal form of Na_2SO_4 (I). Thermal effects given in earlier phase diagrams at 230–280°C arise from reproducible hexagonal ⇔ monoclinic transformations in the metastable region of the phase diagram. The hexagonal form of Na_2SO_4 (I) represents the only stable solid solution. $2Na_2SO_4 \cdot CaSO_4$ [129] indicates a composition of another solid solution series of Na_2SO_4 (I), which is metastable at all temperatures. Depending on the $CaSO_4$ content three metastable forms of solid solutions can be obtained by quenching of melts to room temperature. A transformation scheme into the stable phases was proposed [131].

Glauberite is also obtained from aqueous solutions as are the metastable hydrates $2Na_2SO_4 \cdot CaSO_4 \cdot 2H_2O$ (''labile salt'') and $Na_2SO_4 \cdot 5CaSO_4 \cdot 3H_2O$, the so-called sodium pentasalt already discussed before [46, 108, 132, 133]. *Hill et al.*

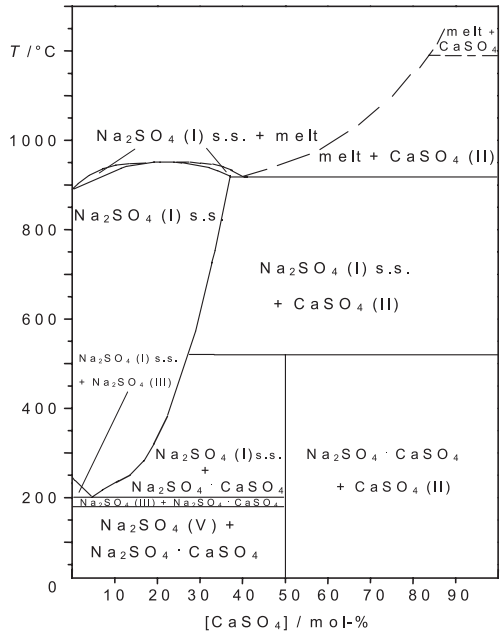

Fig. 13. Phase diagram of the system Na_2SO_4–$CaSO_4$

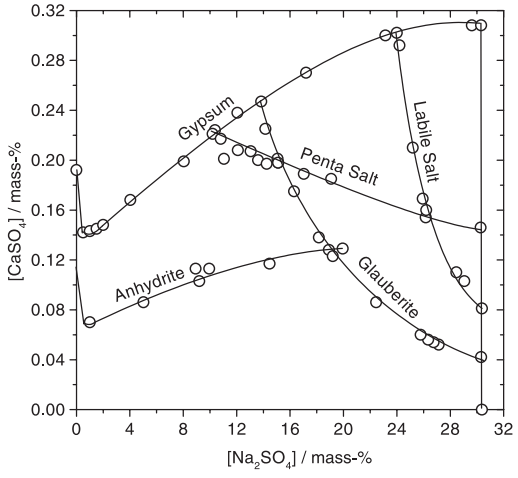

Fig. 14. System Na_2SO_4–$CaSO_4$–H_2O at 75°C [108]

[108] were able to determine the corresponding metastable solubility equilibria at 25, 35, 50, and 75°C (Fig. 14). The same phases occur in the system NaCl–Na_2SO_4–$CaSO_4$–H_2O [134]. The ''labile salt'' was discovered beside glauberite in 1857 by *Fritzsche* [135]. It crystallizes with considerably slow conversion kinetics to the stable phase glauberite [108, 136]. Further, no reproducible ways of forming intermediate hydrates are described in *Vasilevskaya* [137], *Druzhinin* and *Lopina-Shendrik* [138], *Fridman* [139], and *Lopina-Shendrik* [140]. *Emons et al.* [141] postulated the existence of an orthorhombic solid solution causing the different hydrate stoichiometries in literature. Definite conclusions could not be drawn until

now since the very tiny needles are difficult to separate from the mother liquor without decomposition. From combined optical, thermoanalytical and lattice constant determinations *Emons et al.* [141] conclude that mixed crystals with $CaSO_4$:Na_2SO_4 ratios between 1:1.5 up to more than $1:>1.7$ can be formed. The water content of the hydrate $1.6Na_2SO_4{\cdot}CaSO_4{\cdot}x\,H_2O$ is given with x=1.5.

The following minerals are known: eugsterite, $2Na_2SO_4{\cdot}CaSO_4{\cdot}2H_2O$ [142] identical with the ''labile salt''; glauberite; hydroglauberite, $5Na_2SO_4{\cdot}3CaSO_4{\cdot}6H_2O$ [144], also obtained as solid phase in the hexary oceanic salt system at isothermal equilibrations at 25 and 35°C for a long time [144, 145]; wattevillite, $Na_2SO_4{\cdot}CaSO_4{\cdot}4H_2O$ [146], and a hydrate composition of $Na_2SO_4{\cdot}2CaSO_4{\cdot}3H_2O$ was discovered [147]. Also, the different mineral compositions indicate a possible solid solution series. The occurrence of all these minerals in paragenesis with other oceanic salts like gypsum, bassanite, thenardite, halite, astracanite, and glauberite makes an exact composition determination very difficult.

The formation of double salts has been investigated by hydration processes of quenched metastable phases $2Na_2SO_4{\cdot}CaSO_4$ and $4Na_2SO_4{\cdot}CaSO_4$ with water vapour (see above). Hydration of $2Na_2SO_4{\cdot}CaSO_4$ leads to the formation of glauberite and thenardite (Na_2SO_4 V), preceded by the intermediate formation of ''labile salt''. The phase $4Na_2SO_4{\cdot}CaSO_4$ reacts to hydroglauberite and thenardite monitored by gravimetry and X-ray diffraction [148]. Hydration of the known metastable Na_2SO_4–$CaSO_4$ solid solutions in solid–gas (water vapour) reactions as demonstrated in [148] could possibly reveal more details about the hydrate stoichiometries.

Double Salts with Potassium Sulfate

From the phase diagrams [127, 149–153] of the anhydrous system no consistent picture can be derived about the possible stoichiometries of compounds. The existence of $K_2SO_4{\cdot}2CaSO_4$ as the only stable double salt is described uniformly but with disagreements regarding the melting point [127, 149–151]. *Mukinov et al.* [152] reported a possible phase $K_2SO_4{\cdot}3CaSO_4$ and $K_2SO_4{\cdot}CaSO_4$, which should exist below 780°C. *Golubeva et al.* [153] reported a $2K_2SO_4{\cdot}3CaSO_4$ compound with the melting point of 1020°C. To resolve the disagreement *Rowe et al.* [154] performed phase equilibrium studies at high temperatures and found the phase $K_2SO_4{\cdot}2CaSO_4$ (calcium langbeinite) only, which agrees with [127, 149–151].

Calcium langbeinite is well characterised. The thermal effect observed at 936°C remains unclear. According to [154] it does not represent a presumed inversion to a high temperature α-$K_2SO_4{\cdot}2CaSO_4$ denoted in respective phase diagrams in Refs. [127, 149, 151]. At room temperature $K_2SO_4{\cdot}2CaSO_4$ has an orthorhombic lattice and transforms at 200°C into the cubic langbeinite structure ($K_2SO_4{\cdot}2MgSO_4$=parent compound) [155]. At high temperatures both phases can form solid solutions with each other as was shown during the thermal decomposition of polyhalite [156].

Anhydrous potassium–calcium double sulfates do not crystallize from aqueous solutions below 200°C. In the system K_2SO_4–$CaSO_4$–H_2O up to nearly 200°C only the double salts $K_2SO_4{\cdot}CaSO_4{\cdot}H_2O$ (syngenite) and $K_2SO_4{\cdot}5CaSO_4{\cdot}H_2O$ (goergeyite) appear. The concentration range of syngenite along the solubility

isotherms becomes smaller with increasing temperature and that of goergeyite enlarges at the same time [123]. Recently, from determinations of the solubility equilibria in this system up to 200°C it was shown that the maximum temperature of existence of syngenite in contact with aqueous solutions is limited to about 180–190°C. At 200°C and high potassium sulfate concentrations an anhydrous double sulfate occurs for the first time. The composition was determined as $K_2SO_4{\cdot}CaSO_4$. The monoclinic space group $C2/c$ and Z=8 formula units with the lattice parameters a=7.510(2) Å, b=21.856(4) Å, c=9.237(2) Å and β=113.24° were determined. The double salt is isotypic with the palmierite ($K_2SO_4{\cdot}PbSO_4$) and considered as its calcium analog [157]. This again raises the question of the existence field of $K_2SO_4{\cdot}CaSO_4$ in the anhydrous system K_2SO_4–$CaSO_4$.

Syngenite and goergeyite type double salts are also known with NH_4^+ or Rb^+ instead of K^+. As *D'Ans et al.* [136] pointed out variation of the monovalent ion in the series K^+–NH_4^+–Rb^+–Cs^+ decreases the upper temperature limit of hydrate stability in aqueous solutions. Rubidium syngenite exists only below 42°C, for cesium sulfate no hydrous double salt with $CaSO_4$ is known. On the other hand the anhydrous dicalcium salt $Cs_2SO_4{\cdot}2CaSO_4$ of cubic langbeinite type is formed from aqueous solutions already below 0°C [136]. In Table 4 the comparable double salts containing alkaline metal and ammonium ions are listed. With Li_2SO_4 only

Table 4. Calcium sulfate double salts with alkaline metal and ammonium sulfate

	Existence conditions of $X_2SO_4{\cdot}CaSO_4{\cdot}H_2O$, $X_2SO_4{\cdot}5CaSO_4{\cdot}H_2O$ and anhydrous phases			
X	(Syngenite type)	(Goergeyite type)	$X_2SO_4{\cdot}CaSO_4$	$X_2SO_4{\cdot}2CaSO_4$
Li	–	–	–	–
Na	–	($Na_2SO_4{\cdot}5CaSO_4{\cdot}3H_2O$, hemihydrate structure)	from 29°C [136] in aqueous system, at 520°C thermal decomposition [131]	–
K	until about 190°C in aqueous system [157], thermal decomposition at 270°C	from 40°C (31.8°C [158]) enlarging stability field with temperature [123, 157]	at 200°C in aqueous system [157]	until 1011°C in anhydrous system [154]
NH_4	below 25–90°C in aqueous system [136]	17–110°C in aqueous system [136]	–	above 76°C [136] (62°C [159]) in aqueous system
Rb	below 0–42°C [136]	–	–	above 20°C [136], until 1043°C in anhydrous system [127]
Cs	–	–	–	below 0°C, with increasing temperature more stable [136], until 959°C in anhydrous system [127]

one hydrous double salt phase, $x\,Li_2SO_4{\cdot}CaSO_4{\cdot}3H_2O$, is discussed where the mole number x is varying [160]. This phase crystallizes from aqueous solution at enhanced temperatures. At 25°C only the single hydrates $Li_2SO_4{\cdot}H_2O$ and $CaSO_4{\cdot}2H_2O$ crystallize in the ternary system Li_2SO_4–$CaSO_4$–H_2O [161].

Double Salts with Alkaline Earth Metal Sulfates

In aqueous systems nothing is known about double salt formation between $CaSO_4$ and alkaline earth metal sulfate, whereas *Rowe et al.* [162] report a $3MgSO_4{\cdot}CaSO_4$ compound in the melting diagram of the system $MgSO_4$–$CaSO_4$. *Smith et al.* [163] recently detected a compound $2MgSO_4{\cdot}CaSO_4$ in a flue gas filter cake and characterised the double salt by IR spectroscopy and X-ray diffraction.

Polyhalite

The mineral polyhalite represents a triple salt $K_2SO_4{\cdot}MgSO_4{\cdot}2CaSO_4{\cdot}2H_2O$ with wide spread occurrence in evaporitic rock salt formations with average contents of 1–3%. The hydrate water is coordinated at the magnesium ion [164] and therefore water is lost only when heating above 250°C [156, 165]. The salt can be prepared by reaction of gypsum with appropriate solutions in the ternary system K_2SO_4–$MgSO_4$–H_2O at temperatures above 70°C [3, 158]. At lower temperatures polyhalite crystallization becomes slow, at room temperature crystallization was not observed under laboratory conditions. Thus, limits of solution composition for the stable existence of polyhalite at low temperatures could only be proved by dissolution experiments. The most recent investigation of solubility equilibria in the hexary oceanic salt system including the stability field of polyhalite between 35–110°C can be found in Refs. [166, 167]. Surprisingly, *D'Ans* [158] reported a much easier crystallization of the analogous triple salts containing Cu and Ni instead of Mg. He synthesized also the triple salts with the cation combinations K–Zn–Ca, NH_4–Cu–Ca, and NH_4–Cd–Ca and supposed also the substitution by the divalent ions Fe^{2+}, Mn^{2+}, Co^{2+}, and monovalent ions Rb^+ and Cs^+. Later the triple salt with the K–Cu–Ca combination was found as a mineral in Chile and was named Leightonite [168]. Cell dimensions are very similar to polyhalite, however, there is some confusion about the exact crystal symmetry [169].

Conclusions and Outlook

The chemistry of calcium sulfate is dominated by the phases gypsum, $CaSO_4{\cdot}2H_2O$, hemihydrate, $CaSO_4{\cdot}0.5H_2O$, and anhydrite, $CaSO_4$. The extremely slow crystallization kinetics of anhydrite in aqueous solutions at temperatures below 70°C prevent reliable establishment of solubility equilibria from supersaturated solutions. As a consequence uncertainty remains in the anhydrite solubility curve, which gives rise to the corresponding uncertainty of the gypsum–anhydrite conversion temperature in water with best estimates varying between 42–60°C. The calcium sulfate phases give an instructive example that determination of reliable solubility data requires consideration of the substance and phase specific crystallization and transformation kinetics.

Hemihydrate can be formed by dehydration of gypsum in dry solid state or in aqueous solutions at enhanced temperatures. The resulting hemihydrates (β-, α-hemihydrate) show different thermal and hydration characteristics, which cannot be traced back to specific structural features of α- and β-hemihydrate. Despite the importance of knowledge of the α- and β-hemihydrate content in industrial gypsum products its quantitative determination relies exclusively on thermal analysis.

Because of the importance for gypsum-based binder and building materials a number of studies on crystallization and setting kinetics of gypsum have been performed with emphasis on retarding and accelerating effects of additives. No general mechanistic model has been developed until now, which can explain most of the effects observed with respect to kinetics and crystal morphology.

Systematic kinetic investigations on hemihydrate formation in aqueous solutions are missing up to now. Obviously, hemihydrate represents an important intermediate phase during transformation of gypsum into anhydrite. Its open one dimensional channel structure makes ion substitution easier than for gypsum. This yields solid solutions or nearly stoichiometric compounds like the sodium pentasalt. Ion substituted hemihydrates seem to play a role in the crystallization mechanism of anhydrite or double salts like glauberite, goergeyite, or polyhalite precipitating from oceanic salt solutions or brines.

In situ techniques such as FT-Raman spectroscopy or time-resolved X-ray diffraction available for the detection of crystallising phases will provide detailed mechanistic insights in future. Much more emphasis should be given to the crystal chemistry, phase equilibria, and formation kinetics of related phases discussed in this review.

Isomorphous ion substitution (*e.g.* PO_4^{3-}, Ln^{3+}) could be exploited as structural probes in $CaSO_4$ phases applying techniques like optical spectroscopy or nuclear magnetic resonance. On the other hand foreign ion distribution studies between solution and solid sulfate phases would provide the currently lacking quantitative information for assessment procedures of disposal of inorganic toxic and nuclear waste in rock salt formations.

References

[1] Knittel E, Phillips W, Williams Q (2001) Phys Chem Min **28**: 630
[2] Reisdorf K, Abriel W (1988) Zement-Kalk-Gips **41**: 356
[3] D'Ans J (1933) Die Lösegleichgewichte der Systeme der Salze ozeanischer Salzablagerungen. Kali-Forschungs-Anstalt GmbH, Berlin Verlagsgesellschaft für Ackerbau MBH, Berlin SW11
[4] D'Ans J, Bredtschneider D, Eick H, Freund H-E (1954) Kali u Steinsalz **9**: 17
[5] Sborgi U, Bianchi C (1940) Gazz Chim Ital **70**: 823
[6] Hill AE (1937) J Am Chem Soc **59**: 2242
[7] D'Ans J (1968) Kali Steinsalz **5**: 109
[8] Bock E (1961) Can J Chem **39**: 1746
[9] Van't Hoff JH, Armstrong EF, Hinrichsen W, Weigert F, Just G (1903) Z phys Chem **45**: 257
[10] Posnjak E (1938) Amer J Sci **5**(35A): 247
[11] Lange E, Monheim J (1925) Z phys Chem **A150**: 349
[12] Hardie LA (1967) Amer Min **52**: 171
[13] Raju KUG, Atkinson G (1990) J Chem Eng Data **35**: 361
[14] Parker VB, Wagman DD, Evans WH (1971) NBS Tech Note No **270**: 6

[15] Wagman DD, Evans WH, Parker VB, Schumm RH, Halow I, Bailey SM, Churney KL, Nuttal RL (1982) J Phys Chem Ref Data **11** Suppl No 2
[16] Knacke O, Gans W (1977) Z Phys Chem **104**: 41
[17] Barin I, Knacke O, Kubaschewski O (1977) Thermochemical Properties of Inorganic Substances. In: Springer-Verlag Berlin, Heidelberg, New York
[18] Linke WF, Seidell A (1965) Solubilities of Inorganic and Metal Organic Compounds, 4th Ed, Vol 1, 2, Amer Chem Soc, Washington DC
[19] Pel'sh AD (1973) Handbook of experimental solubility data in multi component water-salt systems. vol 1 (1973), vol 2 (1975), Publ Khimiya, Leningrad
[20] Marshall WL, Slusher R (1973) J Chem Thermodyn **5**: 189
[21] Kalyanaraman R, Yeattts LB, Marshall WL (1973) J Chem Thermodyn **5**: 891
[22] Kruchenko VP, Beremzhanov BA (1980) Zh Neorg Khim **25**: 3076
[23] Kruchenko VP (1985) Zh Neorg Khim **30**: 1566
[24] Freyer D (2000) Zur Phasenbildung und -stabilität im System Na_2SO_4–$CaSO_4$–H_2O. Dissertation, TU Bergakademie Freiberg
[25] Monnin C (1990) Geochim Cosmochim Acta **54**: 3265
[26] Monnin C (1999) Chem Geol **153**: 187
[27] Krumgalz BS, Starinsky A, Pitzer KS (1999) J Solution Chem **28**: 667
[28] Mac Donald GJF (1953) Amer J Sci **251**: 884
[29] Krüger R-R, Abriel W (1990) Z Naturforsch **45B**: 1221
[30] Lancia A, Musmarra D, Prisciandaro M (1999) AIChE J **45**: 390
[31] He S, Oddo JE, Tomson MB (1994) J Coll Interfac Sci **162**: 297
[32] Prisciandaro M, Lancia A, Musmarra D (2001) AIChE J **47**: 929
[33] Prisciandaro M, Lancia A, Musmarra D (2001) Ind Eng Chem Res **40**: 2335
[34] He S, Oddo JE, Tomson MB (1994) J Coll Interfac Sci **163**: 372
[35] Hina A, Nancollas GH (2000) In: Alpers ChN, Jambor JL and Nordstrom DK (ed) Reviews in Mineralogy & Geochemistry; Sulfate Minerals, Crystallography, Geochemistry, and Environmental Significance. Mineralogical Society of America, vol 40. Washington, DC, p 277
[36] De Vreugd CH, Witkamp GJ, van Rosmalen GM (1994) J Cryst Growth **144**: 70
[37] Liu ST, Nancollas GH (1975) J Colloid Interfac Sci **52**: 593
[38] Kontrec J, Kralj D, Brecevcic L (2002) J Cryst Growth **240**: 203
[39] Boisvert J-P, Domenech M, Foissy A, Persello J, Mutin J-C (2000) J Cryst Growth **220**: 579
[40] Bertoldi GA (1978) Zement-Kalk-Gips **31**: 626
[41] Konak AR (1976) Krist Tech **11**: 13
[42] Amathieu L, Boistelle R (1987) Chem -IngTech **59**: 858
[43] Badens E, Veesler St, Boistelle R (1999) J Cryst Growth **198**/**199**: 704
[44] Follner S, Wolter A, Preusser A, Indris S, Silber C, Follner H (2002) Cryst Res Technol **37**: 1075
[45] Solberg C, Hansen S (2001) Cem Concr Res **31**: 641
[46] Conley RF, Bundy WM (1958) Geochim Cosmochim Acta **15**: 57
[47] Kushnir J (1980) Geochim Cosmochim Acta **44**: 1471
[48] Witkamp GJ, Rosmalen GM (1991) J Cryst Growth **108**: 89
[49] Curry NA, Jones DW (1971) J Chem Soc **A**: 3725
[50] Aslanian S, Stoilova D, Petrova R (1980) Z anorg allg Chem **465**: 209
[51] Sakae T, Nagata H, Sudo T (1978) Am Mineral **63**: 520
[52] Xu J, Butler IS, Gilson DFR (1999) Spectrochim Acta **A55**: 2801
[53] Rinaudo C, Lanfranco AM, Boistelle R (1996) J Cryst Growth **158**: 316
[54] Hina A, Nancollas GH, Grynpas M (2001) J Cryst Growth **223**: 213
[55] Zdukos AT, Vaimakis TK (1985) Russ J Inorg Chem **30**: 1124
[56] Haerter M (1971) Tonind-Ztg **95**: 9
[57] Ferraris G, Jones DW, Yerkess I (1971) Acta Cryst **B27**: 349

[58] Krüger R-R, Abriel W (1991) Acta Cryst **C47**: 1958
[59] Selivanova NM, Shneider VA (1959) Izv Vyssh Ucheb Zav Khim Khim Tekhnol **2**: 651
[60] Selivanova NM, Shneider VA (1958) Nauch Dokl Vyssh Shk Khim Khim Tekhnol 664
[61] Kohlmann M, Sowa H, Reithmayer K, Schulz H, Krüger R-R, Abriel W (1994) Acta Cryst **C50**: 1651
[62] Ben Amor M, Louer M, Le Marouille JY (1982) CR Seances Acad Sci **2**: 294
[63] Gmelins Handbuch der Anorganischen Chemie. (1962) 8 Aufl, vol 52, Verlag Chemie GmbH, Weinheim
[64] Cooper MA, Hawthorne FC (1996) Can Mineral **34**: 99
[65] Tiemann H, Sötje I, Jarms G, Paulmann C, Epple M, Hasse B (2002) J Chem Soc, Dalton Trans, 1266
[66] Flörke OW (1952) Neues Jb Mineral Abh **4**: 189
[67] Eipeltauer E (1958) Tonind-Ztg **6**: 264
[68] McAdie HG (1965) Can J Chem **42**: 792
[69] Kuntze RA (1965) Can J Chem **43**: 2522
[70] Murat M, Comel C (1971) Tonind-Ztg **95**: 29
[71] Wiedemann HG (1975) Z Anal Chem **276**: 21
[72] Hummel H-U, Abdussaljamow B, Fischer H-B, Stark J (2001) Zement-Kalk-Gips **54**: 272
[73] Heide K (1969) Silikattech **20**: 232
[74] Kurpiers K (1970) Untersuchungen der Entwässerung von Gips bei niedrigen Wasserdampfpartialdrücken. Dissertation TU Clausthal 1970
[75] Oetzel M, Heger G, Koslowski T (2000) Zement-Kalk-Gips **53**: 354
[76] Bobrov BS, Romaschkov AB, Andreva EP (1987) Zh Neorg Khim **23**: 497
[77] Schwotzer M, Weidler PG, Nüesch R (2002) 3. Marburger Gipstagung Phillips-Universität Marburg
[78] Pritzel C, Trettin R (2002) 3. Marburger Gipstagung Phillips-Universität Marburg
[79] Dorozhkin SV (1996) Scanning **18**: 119
[80] Koslowski Th, Ludwig U (1999) Zement-Kalk-Gips **5**: 274
[81] Goto M (1966) Aust J Chem **19**: 313
[82] Powell DA (1958) Nature **182**: 792
[83] Morris RJ (1963) Nature **198**: 1298
[84] Tpiollier M, Guilhot B (1976) Cement and Concrete Res **6**: 507
[85] Galtier P, Soustelle M, Guilhot B (1983) Cement and Concrete Res **13**: 703
[86] Kuzel H-J (1987) N Jb Min, Abh **156**: 155
[87] Robert J, Morris J (1963) Anal Chem **35**: 1489
[88] Wiegel E, Kirchner HH (1966) Ber Dtsch Keram Ges **43**: 718
[89] Lager GA, Armbruster Th, Rotella FJ, Jorgensen JD, Hinks DG (1984) Am Min **69**: 910
[90] Bensted, Prakash S (1968) Nature **219**: 60
[91] Cliffton JR (1971) Phys Sci **232**: 125
[92] Lehmann H, Rieke K (1973) Tonind-Ztg **97**: 157
[93] Lehmann H, Rieke K (1974) Tonind-Ztg **98**: 81
[94] Reisdorf K, Abriel W (1987) N Jb Min, Abh **157**: 44
[95] Budnikov PO, Kosyreva ZS (1953) Voprosy Petrograf i Minera Akad Nauk SSSR **2**: 342
[96] Eipeltauer E (1956) Zement-Kalk-Gips **9**: 501
[97] Southard JC (1940) Ind Eng Chem **32**: 442
[98] Kuzel H-J, Hauner M (1987) Zement-Kalk-Gips **12**: 628
[99] Bushuev NN, Borisov VM (1982) Russ J Inorg Chem **27**: 341
[100] Schneider J, Freyer D, Voigt W (2002) 3. Marburger Gipstagung Phillips-Universität Marburg
[101] Bushuev NN (1982) Zh Neorg Khim **27**: 610
[102] Abriel W, Nesper R (1993) Z Krist **205**: 99
[103] Abriel W (1983) Acta Cryst **C36**: 956

[104] Bezou C, Nonat A, Mutin J-C, Christensen AN, Lehmann MS (1995) J Solid State Chem **117**: 165
[105] Frik M, Kuzel H-J (1982) Fortschr Miner **60**: 79
[106] Gallitelli P (1933) Periodico Mineral Roma **4**: 1
[107] Ballirano P, Maras A, Meloni S, Caminiti R (2001) Eur J Mineral **13**: 985
[108] Hill AE, Will JH (1938) J Amer Chem Soc **60**: 1647
[109] Freyer D, Reck G, Bremer M, Voigt W (1999) Monatsh Chem **130**: 1179
[110] Powell DA (1962) Austr J Chem **15**: 868
[111] Sugimoto K (1958) Asahi Garasu Kenkyu Hokoku **8**: 32
[112] Autenrieth H (1958) Kali u Steinsalz **2**: 181
[113] Gudowius E, von Hodenberg R (1979) Kali u Steinsalz **7**: 501
[114] Freyer D, Ziske S, Voigt W (2002) Freib Forschh **E3**: 127
[115] Takahashi S, Seki M, Setoyama K (1993) Bull Chem Soc Jpn **66**: 2219
[116] Bushuev N, Nabiev AG (1988) Zh Neorg Khim **33**: 2962
[117] Bushuev NN, Nabiev AG, Petropavlovskii IA, Smirnova IS (1988) Zh Neorg Khim **61**: 2153
[118a] Blackburn AV, Gerkin RE (1995) Acta Cryst. **C51**: 2215
[118b] Blackburn AV, Gerkin RE (1994) Acta Cryst. **C50**: 835
[119] Melikhov IV, Berdonosova DG, Fadeev VV, Burlakova EV (1991) Zh Prikl Khim **64**: 334
[120] Lyer PN, Natarajan PR (1989) J Less-Common Met **146**: 161
[121] Kolcu O, Zumreoglu-Karan B (1994) Thermochim Acta **240**: 185
[122] Koopman C, Witkamp GJ (2000) Hydrometal **58**: 51
[123] Hill AE (1934) J Am Chem Soc **56**: 1071
[124] Ostroff AG (1964) Geochim Cosmochim Acta **28**: 1363
[125] Zen E-A (1965) J Petrol **6**: 124
[126] Calcagni G, Mancini G (1910) Atti Linc **19 II**: 426
[127] Müller H (1910) N Jb Min, Beilagebd **30**: 1
[128] Komissarova LN, Plyushev VE, Stepina SB (1955) Tr Mosk Inst Tonkoi Khim Tekhnol **5**: 3
[129] Speranskaja EI, Baraskaja IB (1961) Zh Neorg Khim **6**: 1392
[130] Bandaranayake PWSK, Mellander B-E (1988) Solid State Ionics **26**: 33
[131] Freyer D, Voigt W, Köhnke K (1998) Eur J Solid State Inorg Chem **35**: 595
[132] van't Hoff JH (1905) Ber Berl Akad 478
[133] Barre M (1911) Ann Chim Phys **24**: 162
[134] Rogosowskaya MS, Konontschuk TI, Lukjanowa NK (1980) Zh Neorg Khim **25**: 1095
[135] Fritzsche J (1857) J prakt Chem **72**: 291
[136] D'Ans J, Schreiner O (1909) Z anorg allg Chem **62**: 129
[137] Vasilevskaya AG (1959) Izvest Sib Otd Akad Nauk SSSR **1**: 76; CA 53 (1959) 71687
[138] Druzhinin S, Lopina-Shendrik MD (1962) Izv Akad Nauk Kirg SSR Ser Estestr i Tekknol Nauk **4**: 61; CA 59 (1963) 400552
[139] Fridman YD, Zinov'ev AA, Bogdanovskaya RZ (1953) Tr Inst Khim Kirgiz Filial Akad Nauk SSSR **5**: 49; CA 50 (1956) 87989
[140] Lopina-Shendrik MD (1958) Tr Molodykh Nauchn Rabot Akad Nauk Kirg SSR: 43; CA 55 (1961) 50869
[141] Emons H-H, Seyfarth H-H, Stegmann E (1971) Krist u Tech **6**: 85
[142] Vergouen L (1981) Am Min **66**: 632
[143] Sljusareva MN (1969) Zap vses mineralog Obsc **98**: 59
[144] Gu S, Lin H (1985) Kexue Tongbao **30**: 1375
[145] Gu S, Lin H (1986) Kexue Tongbao **31**: 624
[146] Fejer E, Cressey G (1988) British Museum, London, England, UK, JSPDS Grant-in-Aid, Report
[147] Hodenberg R, Miotke F-D (1983) Kali Steinsalz **8**: 374
[148] Freyer D, Fischer St, Köhnke K, Voigt W (1997) Solid State Ionics **96**: 29

[149] Graham W (1913) Z Anorg Chem **81**: 257
[150] Jänecke E, Mühlhäuser W (1936) Z anorg allgem Chem **228**: 241
[151] Bellanca A (1942) Periodico Mineral (Rome) **13**: 21
[152] Mukinov SM, Krylova NI, Bergman AG (1949) Tr Inst Khim Akad Nauk Uz SSR Inst Khim Obshch i Neorg Khim **2**: 94
[153] Golubeva MS, Bergman AG (1956) Zh Obshch Khim **26**: 328
[154] Rowe JJ, Morey GW, Hansen ID (1965) J Inorg Nucl Chem **27**: 53
[155] Morey GW, Rowe JJ, Fournier RO (1964) J Inorg Nucl Chem **26**: 53
[156] Fischer St, Voigt W, Köhnke K (1996) Cryst Res Technol **31**: 87
[157] Freyer D, Voigt W (2003) accepted for publication in Cosmochim Geochim Acta
[158] D'Ans J (1908) Chem Ber **41**: 1776
[159] Hill AE, Yanick NS (1935) J Am Chem Soc **57**: 645
[160] Petrova MI, Alymkulova KS, Dzhashakueva BK, Kydynov MK (1981) Deposited Doc, VINITI: 2357, USSR; CA 97 (1982) 616657
[161] Kydynov MK, Petrova MI (1965) Zh Prikl Khim **38**: 2590
[162] Rowe JJ, Morey GW, Silber CC (1967) J Inorg Nucl Chem **29**: 925
[163] Smith DH, Seshadri KS, (1999) Spectrochimica Acta **A**(55): 795
[164] Schlatti M, Sahl K, Zemann A, Zemann J (1970) Tschermaks Mineralog Petrogr Mitt **14**: 75
[165] Jockwer N (1981) Kali Steinsalz **8**: 126
[166] Kropp E, Beate R, Grosch Ch, Kranz M, Holldorf H (1988) Freib Forschh **A764**: 42
[167] Kropp E, Holldorf H (1988) Freib Forschh **A764**: 67
[168] Palache Ch (1938) Am Mineral **23**: 34
[169] Hawthorne FC, Krivovichev SV, Burns PC (2000) In: Alpers ChN, Jambor JL, Nordstrom DK (eds) Reviews in Mineralogy & Geochemistry; Sulfate Minerals, Crystallography, Geochemistry, and Environmental Significance. Mineralogical Society of America, vol 40 Washington, DC, p 1